Photo-Ionization Cross Sections of the Elements Helium to Xenon*

Eugene J. McGuire
Sandia Laboratory, Albuquerque, New Mexico
(Received 22 May 1968)

The quantity $-rV(r)$ calculated by Herman and Skillman, using the Hartree-Fock-Slater approach, is approximated by a series of straight lines. With such a potential the radial Schrödinger equation is exactly solvable with Whittaker functions. The bound-state eigenvalue equation is found and is used to adjust the parameters of the straight lines so that the model eigenvalues and those of Herman and Skillman are in reasonable agreement. With the discrete and continuum orbitals of the model, the photo-ionization cross section for all the shells of the elements helium–xenon are computed.

I. INTRODUCTION

In a previous paper[1] the photo-ionization cross sections for some shells of some atoms were computed using the exact continuum solutions to a crude atomic model. The single-model parameter was chosen by comparing the discrete eigenvalues of the model with experimental data. In this paper, the model of Ref. 1 is considerably expanded, the number of parameters is made dependent on the size of the atom, and the parameters are chosen so that the calculated eigenvalues are in reasonable agreement with computed Hartree-Fock-Slater values.[2] The new model leads to accurate orthonormal orbitals for all the filled shells as well as the continuum, and affords the opportunity to compute the photo-ionization cross section for all the atomic shells, within the approximations made in the photo-ionization matrix elements (Sec. III).

The only other approach that has been extensively applied for calculating these cross sections is to use the hydrogenic expressions[3] with suitably chosen effective charges. In using the hydrogenic expressions, one employs the regular confluent hypergeometric functions only.[4] In our model, both regular and irregular functions are allowed. Both Salpeter and Zaidi[5] and Cooper[6] have calculated photo-ionization cross sections over a wide spectral range, but this was limited to the outer electron in the atom. Recently Manson and Cooper[7] computed the photo-ionization cross section for several shells of some heavy elements in the soft x-ray region. Our calculations and those of Manson and Cooper start with the Herman-Skillman[2] central field, but where Manson and Cooper determine the continuum orbitals by numerical integration, we approximate the central potential and find the exact continuum orbitals for the approximate potential.

Our aim in performing these calculations was threefold: first, to provide calculations where none were available; second, to provide a framework wherein measurements made in different spectral regions can be compared; and third, to see how accurately the calculations could be made given the assumptions used to compute the relevant matrix elements, and to determine what corrections might be made when calculation and experiment disagreed.

II. THE MODEL

The radial Schrödinger equation, in Rydberg units, with an effective central potential is

$$\left(\frac{d^2}{dr^2} - \frac{2Z(r)}{r} - \frac{l(l+1)}{r^2} + E\right)\phi(E, l; r) = 0. \quad (1)$$

$Z(r)$ is a function which decreases monotonically from Z at $r=0$ to z at $r=\infty$, where, for the system in question, Z is the charge on the nucleus and z is the charge on the residual ion ($z=1$ for a neutral system). In the model we approximate $Z(r)$ by a series of straight lines

$$Z(r) = Z_i - \Delta_i r/2; \quad r_{i-1} \leq r \leq r_i; \quad i = 1, n \quad (2)$$

with $r_0 = 0$, Z the nuclear charge, $r_n = \infty$, $Z_n = z$, and $\Delta_n = 0$. The potential is continuous which requires

$$2(Z_i - Z_{i+1}) = (\Delta_i - \Delta_{i+1})r_i \,. \quad (3)$$

The derivative of the potential is not continuous, but this is not expected to affect the one-electron orbitals.[8] We have a number of unknown parameters Z_i, Δ_i, and r_i. However, we reduce the number of unknowns to one by fitting the straight lines to the charge $Z(r)$. The parameter r_{n-1} is then approximately chosen, and we refine the choice by varying r_{n-1} so that the eigenvalue for the outermost filled orbital agrees exactly with that of Herman and Skillman.[2] Then, with all the parameters established, we compute the model eigenvalues for all the other filled orbitals. If each of these agrees with those of Herman and Skillman to better than 10%, we consider the model to be a good approximation; if not, we repeat the process. The figure 10% is arbitrary, and presumably one could use 441 straight-line segments[9] to exactly reproduce the Herman-Skillman effective charge. We chose 10% to use the minimum number of straight-line segments consistent with reasonable accuracy.

The radial Schrödinger equation is then

$$\left(\frac{d^2}{dr^2}+\frac{2Z_i}{r}-\Delta_i-\frac{l(l+1)}{r^2}+E\right)\phi_i(E,l;r)=0;$$

$$r_{i-1}\leq r\leq r_i\ . \quad (4)$$

For $E<0$, the solutions satisfying the boundary conditions at zero and infinity are[10]

$$\phi_1(E,l;r)=A_1\phi_{1,1},$$

$$\phi_i(E,l;r)=A_i(\phi_{1,i}+B_i\phi_{2,i})\ ;\quad 2\leq i\leq N-1,$$

$$\phi_N(E,l;r)=B_N\phi_{2,N},$$

where $\phi_{1,i}=M_{\alpha_i,\,l+\frac{1}{2}}(2rZ_i/\alpha_i)$,

$$\phi_{2,i}=\Gamma(l+1-\alpha_i)W_{\alpha_i,\,l+\frac{1}{2}}(2rZ_i/\alpha_i)$$

and $\alpha_i=Z_i(\Delta_i+|E|)^{-1/2}$. (5)

Matching solutions and their derivatives at the boundaries leads to the eigenvalue equation:

$$B_2=-[\phi_{1,1},\phi_{1,2}]/[\phi_{1,1},\phi_{2,2}],$$

$$B_{i+1}=-\frac{[\phi_{1,i},\phi_{1,i+1}]+B_i[\phi_{2,i},\phi_{1,i+1}]}{[\phi_{1,i},\phi_{2,i+1}]+B_i[\phi_{2,i},\phi_{2,i+1}]}\ ;$$

$$2\leq i\leq N-2,$$

$$[\phi_{1,N-1},\phi_{2,N}]+B_{N-1}[\phi_{2,N-1}\phi_{2,N}]=0, \quad (6)$$

where

$$[f(ax),g(bx)]=(fdg/dx-g\,df/dx)\big|_{x=x_0}.$$

For $E>0$ and $\Delta_j\leq E\leq\Delta_{j-1}$ the solutions are those given above for $i<j$, while for $i\geq j$, they are

$$\phi_i=A_i[G_l(2rz_i,-1/\eta_i^2)+B_iH_l(2rz_i,-1/\eta_i^2)],\ j\leq i\leq N,$$

where $\eta_i=Z_i(E-\Delta_i)^{-1/2}$. (7)

Normalizing the solution so that

$$\lim_{r\to\infty}\phi(E,l;r)=(\eta_N/\pi z)^{1/2}\cos[rz/\eta_N+\eta_N\ln(2rz/\eta_N)-\pi(l+1)/2+\arg\Gamma(l+1-i\eta_N)+\sigma_l]\ , \quad (8)$$

one can explicitly evaluate all the A_i and B_i. These exact, orthonormal continuum functions are the motivation for approximating the central potential.

III. THE PHOTO-IONIZATION CROSS SECTION

In the model developed in Sec. II, the orbitals are all eigenfunctions of a common central potential. This also occurs in the Hartree-Fock-Slater approach of Herman and Skillman.[2] In the latter case, the field is self-consistent while the solutions are obtained by numerical integration, while in the former, the solutions are not self-consistent but are exact. However, both use a common central potential. Thus, in addition to assuming an independent-particle model, we assume the independent particles are described by eigenfunctions of a common central field. This is an assumption with regard to the model, not merely with regard to the photo-ionization matrix element. As we shall see, when comparing calculation and experiment for the heavier elements near the outer-shell (i.e., $3p$ in argon, $3d$ and $4p$ in krypton, and $4d$ and $5p$ in xenon) thresholds, there is serious disagreement both in cross-section magnitude and shape. Cooper and Manson,[7] with the same independent-particle, common-central-field approach, but with numerically integrated continuum orbitals, compute cross sections close to ours so the discrepancy does not lie in our approximation to the Herman-Skillman potential. The assumptions made about the photo-ionization matrix element, *per se*, are valid near these thresholds. Thus, it appears that the independent-particle model, common central-field assumption is poor for these cases.

In calculating the photo-ionization matrix element, we assume that an unrelaxed core treatment is sufficient,[6] and that the dipole approximation is satisfactory over the wide spectral range treated. In the unrelaxed core approximation, we assume Koopman's theorem[11] so that the overlap integrals between passive electrons in the initial and final states are unity, and the one-electron eigenvalue is the ionization energy. This assumption is questionable in some situations (e.g., the precise determination of x-ray thresholds[12]), but a comparison of the calculations reported in Sec. IV with experiment over a wide spectral range in no significant way discredits this assumption. For example, for incident photon energies greater than the K-shell ionization threshold in copper there is no discrepancy between calculation and experiment indicating the calculated cross section should be reduced by a core-relaxation factor.

The computations presented in Sec. IV cut off at

an energy roughly ten times the K-shell ionization energy. The dipole approximation for a particular shell transition is expected to break down at higher energies. However, for the outer shells the cross section is small when this occurs and other shells, not affected by the breakdown of the dipole approximation, provide the dominant cross section; while for energies higher than the K-shell ionization the calculation is cut off. Thus the dipole approximation is expected to be valid over the range of photon energies treated here.

Finally, throughout the calculations we use the dipole-length formulation of the matrix element. Since the orbitals used are exact, one expects the dipole length, dipole velocity, and dipole acceleration formulations to lead to the same result. With these assumptions the photo-ionization cross section for an atomic shell is[1]

$$\sigma_\nu = 8.56 \times \pi \times 10^{-19} E \sum_{l'=l\pm1} C_{l'} \times \left| \int_0^\infty \phi(-E_0, l; r) r \phi(\epsilon, l'; r)\, dr \right|^2, \quad (9)$$

where ν is the photon frequency, $h\nu = E = \epsilon + E_0$. The cross section is in cm^2 when E is in rydbergs and the continuum orbital is normalized as in Eq. (8). Generally, in these calculations, we neglect term splitting so $C_{l'} = N_q \max(l, l')/(2l+1)$ where N_q is the number of electrons in the shell in question in the ground state. Only in the case of oxygen do we attempt to account for term-splitting effects. Equation (9) is modified to

$$\sigma_\nu = 8.56\pi \times 10^{-19} \sum_L [\epsilon + E_{\text{expt}}(L)] \times \sum_{l'=l\pm1} C_{l'}(L) \left| \int_0^\infty \phi(-E_0, l; r) r \phi(\epsilon, l'; r)\, dr \right|^2,$$

where $E_{\text{expt}}(L)$ is the experimental continuum threshold for a particular final configuration term and $C_l(L)$ is the appropriate coefficient.[13] The matrix element used is that calculated with no term splitting.

IV. THE CALCULATED CROSS SECTIONS

The number of straight-line segments in the model increased in going up the periodic table (four for He-Na, five for Mg-K, six for K-Kr, and seven for Rb-Xe). In Table I, we list the model parameters for eight of the elements, and in Table II, the model and Herman-Skillman eigenvalues for the occupied levels. In Table II the model eigenvalue is listed above the Herman-Skillman value.

It can be seen in Table II that for some eigenvalues (e.g., Cu 3d) we did not meet the criterion that the two sets of eigenvalues agree to 10%. This occurs for partially filled d shells. Parameter variation indicated that in such cases we could meet the 10% criterion only by adding another segment. Since this was not required when the relevant d shell was filled, we accepted the criterion violation. However, for the elements ments K-Xe, we were able to choose Δ_1 to be approximately $Z^2 - E_{\text{HS}}$, i.e., the internal screening constant.[3] For the 1s shell the difference between the two eigenvalues is then less than 3%.

In regard to the sensitivity of the calculated cross sections to the model parameters, we list the cross section for K twice, calculated with five and six straight lines in the model. It can be seen that this does not significantly affect the cross sections. In general one can say that for the cross section as a function of threshold energy, it rises at threshold with threshold energy. As an example, we show in Fig. 1 the cross section for argon near the K edge and the measurements of Wuilleumier.[14] Wuilleumier indicates that the edge is at -240 Ry. The model edge is at -228 Ry. By varying the model parameters to fit the experimental threshold (neglecting the outer eigenvalues), the calculated cross section is brought into excellent agreement with the measurement.

In Tables III–VIII we list the calculated cross sections for the elements He-Xe.[15] The cross sections are in megabarns (10^{-18} cm^2).

In Fig. 2 we show the calculated cross section for 0, both without term splitting (A) and with term splitting (B), and the measurements of Samson and Cairns.[16] Dalgarno *et al.*[17] used a Hartree-Fock treatment for partially filled shells to compute the oxygen cross section. Our calculation is in good agreement with their dipole-velocity calculation over most of the spectral range, but at threshold it is in better agreement with their dipole-length calculation.

In Fig. 3 we show the calculated cross section of Ne and the measurements of Ederer and Tomboulian[18]

TABLE I. Model parameters for selected elements.

Element	Z_1	Z_2	Z_3	Z_4	Z_5	Z_6	Z_7	R_1	R_2	R_3	R_4	R_5	R_6
O	8.0	6.0	3.5	1.0				0.276	0.830	1.66			
Ne	10.0	7.50	4.0					0.198	0.693	1.49			
Al	13.0	9.4	4.5	2.0	1.0			0.170	0.730	1.93	3.27		
Ar	18.0	13.0	6.8	3.0	1.0			0.140	0.640	1.60	2.61		
Cu	29.0	22.0	15.0	6.8	3.2	1.0		0.110	0.380	0.800	1.55	2.26	
Kr	36.0	27.7	16.25	6.95	3.0	1.0		0.090	0.364	0.900	1.87	3.32	
Ag	47.0	38.0	26.0	15.0	7.0	3.0	1.0	0.075	0.240	0.600	1.20	1.95	2.96
Xe	54.0	47.0	27.0	14.6	6.70	3.00	1.0	0.063	0.300	0.690	1.22	2.28	3.58

TABLE II. Model and Herman-Skillman eigenvalues for the occupied levels:

Element	E_{1s}	E_{2s}	E_{2p}	E_{3s}	E_{3p}	E_{3d}	E_{4s}	E_{4p}	E_{4d}	E_{5s}	E_{5p}
O	-41.1	-2.20	-1.04								
	-39.5	-2.14	-1.04								
Ne	-61.2	-3.23	-1.47								
	-63.0	-3.17	-1.47								
Al	-112.0	-9.40	-6.38	-0.797	-0.358						
	-113.7	-8.72	-5.95	-0.745	-0.358						
Ar	-228.7	-23.9	-18.1	-2.25	-1.065						
	-232.5	-22.9	-18.2	-2.11	-1.065						
Cu	-664.2	-80.0	-68.1	-8.85	-5.61	-0.926	-0.509				
	-649.7	-78.2	-69.0	-8.63	-5.71	-0.743	-0.509				
Kr	-1052.	-130.2	-112.5	-19.3	-14.4	-7.25	-1.99	-0.952			
	-1031	-135.5	-123.3	-19.7	-15.3	-7.10	-1.95	-0.952			
Ag	-1815	-249	-225	-47.5	-39.2	-25.9	-6.93	-4.34	-1.00	-0.472	
	-1815	-264	-246	-48.9	-41.7	-28.3	-6.93	-4.62	-0.930	-0.472	
Xe	-2434	-371	-342	-80.3	-65.7	-48.4	-13.4	-10.04	-5.17	-1.58	-0.837
	-2434	-372	-351	-76.9	-67.9	-51.0	-14.2	-10.92	-5.26	-1.60	-0.837

and Samson.[19] Calculation and experiment are in excellent agreement.

In Fig. 4 we show the calculated cross section for Ar, the measurements of Samson,[20] of Lukirskii and Zimkina,[21] and a point from Allen's tabulation.[22] The calculated $3p$-ϵd cross section is in good agreement with that of Cooper and Manson.[7]

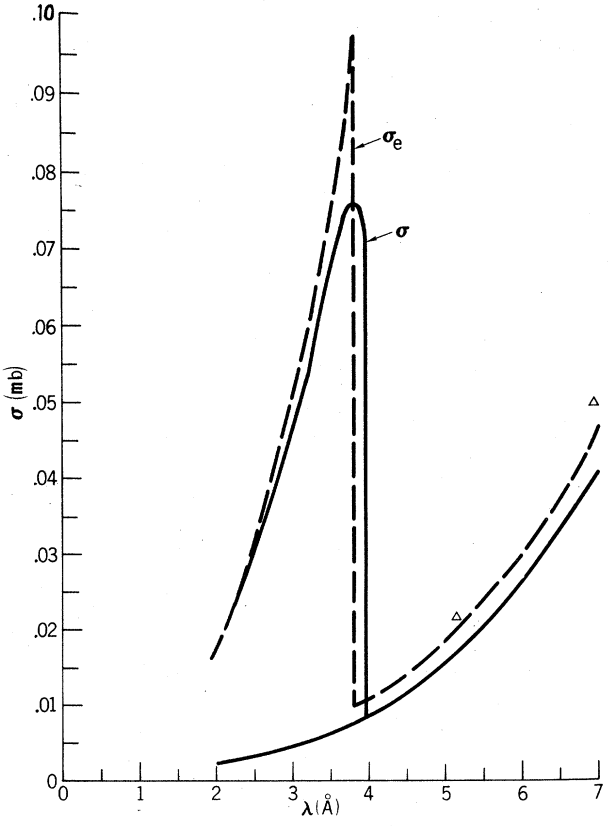

Fig. 1. The photo-ionization cross section of Ar from 2 to 7Å. The dashed curve is from Ref. 14.

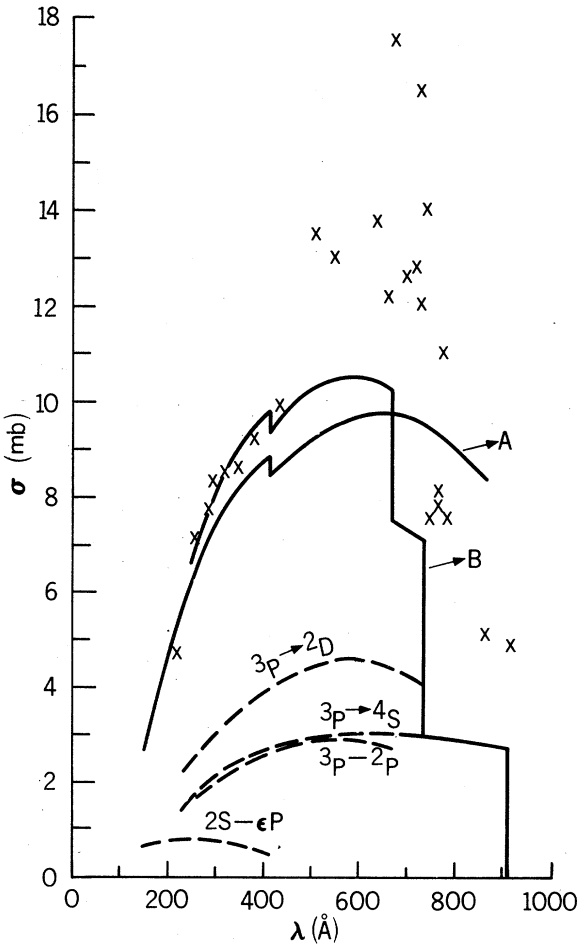

Fig. 2. The photo-ionization cross section of O from 200 to 900 Å. The crosses are from Ref. 16. Curve *A* is the central-field calculation, while curve *B* includes the effect of term splitting.

TABLE III. Calculated cross sections for the elements He–Na

λ (Å)/Element	He	Li	Be	B	C	N	O	Fl	Ne	Na
2000		1.43								0.007
1500		1.48	1.50	8.9						0.038
1200		1.32	2.02	6.4	12.6					0.090
1000		1.10	2.18	4.8	11.2	11.95				0.110
800		0.820	2.02	5.4	9.1	11.9	9.00			0.105
600		0.500	1.60	4.0	7.3	9.65	9.65		5.85	0.0890
400	4.83	0.230	0.98	2.3	4.4	7.80	8.75	10.6	8.80	0.0600
300	2.70	0.130	0.67	1.53	2.9	5.40	7.42	10.1	8.70	5.30
200	1.10	3.35	0.36	0.82	1.45	2.90	4.65	6.7	7.30	8.15
150	0.600	2.40	0.22	0.48	0.88	1.75	2.70	4.1	5.60	6.50
120	0.340	1.52	0.13	0.29	0.590	11.10	1.77	2.6	4.00	4.95
100	0.180	0.980	2.16	0.185	0.400	00.650	1.12	1.8	2.80	4.00
80	0.100	0.580	1.33	0.105	0.240	0.390	0.700	1.3	1.75	2.40
60	0.046	0.285	0.67	1.32	0.108	00.208	0.385	0.59	0.910	1.10
40	0.015	0.089	0.22	0.48	0.81	0.070	0.160	0.245	0.360	0.370
30		0.038	0.118	0.22	0.45	0.680	0.065	0.124	0.170	0.186
20		0.010	0.040	0.080	0.182	00.255	0.395	0.050	0.063	0.075
15			0.018	0.038	0.085	0.125	0.195	0.305	0.030	0.035
12			0.010	0.025	0.047	0.075	0.120	0.170	0.205	0.018
10					0.029	0.047	0.072	0.115	0.135	0.232
8					0.015	0.026	0.041	0.067	0.077	0.138
6						0.012	0.020	0.030	0.039	0.061

However, both are higher than experiment at threshold by almost a factor of 2, and both drop off more rapidly with decreasing wavelength than Samson's measurements. Yet between 10 and 250Å the calculation is in excellent agreement with the measurements of Lukirskii and Zimkina, indicating that for energies higher than that of the first zero in the $3p$-ϵd matrix element the calculation is essentially correct.

In Fig. 5 we show the calculated cross section of

TABLE IV. Calculated cross sections for the elements Mg–K.

λ(Å)/Element	Mg	Al	Si	P	S	Cl	Ar	K
2000		11.4						0.023
1500	0.280	4.9	30.0					0.050
1200	0.027	2.2	17.5	39.0	59.5			0.061
1000	0.040	1.0	7.0	25.0	50.5			0.063
800	0.125	0.33	1.80	8.50	28.0	59.0	60.0	0.057
600	0.182	0.31	0.50	1.20	4.20	11.0	52.5	0.043
400	0.192	0.45	0.57	0.68	0.85	1.35	2.00	4.00
300	0.152	0.45	0.60	0.84	1.00	1.07	1.00	1.20
200	4.30	0.34	0.55	0.84	1.17	1.35	1.52	1.85
150	7.35	0.25	0.46	0.77	1.02	1.22	1.52	1.92
120	6.65	6.48	0.36	0.57	0.85	1.00	1.33	1.88
100	4.80	5.50	5.24	0.47	0.70	0.82	1.10	1.52
80	3.10	4.13	4.62	5.40	0.50	0.60	0.85	1.20
60	1.65	2.55	3.10	3.46	3.60	6.40	0.55	0.67
40	0.68	1.05	1.36	1.70	2.05	2.45	2.52	3.70
30	0.36	0.51	0.68	0.85	1.12	1.40	1.66	2.0
20	0.125	0.185	0.245	0.30	0.39	0.45	0.62	0.74
15	0.060	0.090	0.115	0.15	0.18	0.22	0.29	0.36
12	0.035	0.048	0.063	0.080	0.10	0.123	0.16	0.20
10	0.0240	0.0265	0.0375	0.051	0.070	0.079	0.10	0.125
8	0.152	0.170	0.0212	0.0305	0.0380	0.047	0.060	0.070
6	0.079	0.058	0.108	0.0125	0.0164	0.0195	0.026	0.0325
4	0.0275	0.0335	0.0445	0.055	0.067	0.075	0.0085	0.0105
3	0.0134	0.0175	0.0205	0.027	0.034	0.039	0.046	0.056

TABLE V. Calculated cross sections for the elements K–Co.

λ(Å)	K	Ca	Sc	Ti	V	Cr	Mn	Fe	Co
2000	0.015	0.62	0.50			0.60			
1500	0.047	0.025	2.20	2.90	0.22	6.60	1.25	1.40	1.20
1200	0.061	0.015	2.58	3.20	2.45	7.35	0.40	0.40	0.45
1000	0.066	0.06	2.98	3.52	3.15	7.85	0.02	0.06	0.10
800	0.058	0.10	3.25	4.00	4.05	8.40	0.02	0.01	0.00
600	0.047	0.13	3.27	4.67	5.45	8.85	2.70	2.95	3.45
400	3.30	0.14	2.50	4.26	5.98	9.20	5.25	5.40	5.90
300	1.45	1.40	4.80	3.70	5.42	8.25	7.05	7.25	7.85
200	1.80	1.85	2.35	3.34	4.92	7.10	8.20	7.90	8.85
150	1.80	2.05	2.08	3.03	3.90	5.30	6.60	7.40	8.50
120	1.50	1.80	1.95	2.551	3.20	4.15	5.45	6.00	6.80
100	1.30	1.53	1.67	2.32	2.70	3.30	4.45	5.05	5.55
80	1.03	1.16	1.25	1.70	2.05	2.40	3.30	3.90	4.10
60	0.68	0.78	0.78	1.02	1.22	1.45	2.05	2.50	2.55
40	3.30	0.43	0.43	0.48	0.55	0.72	0.98	1.10	1.25
30	1.92	2.20	2.50	0.32	0.35	0.45	0.60	0.63	0.65
20	0.73	0.92	1.20	1.40	1.55	0.20	0.25	0.26	0.36
15	0.40	0.50	0.68	0.74	0.80	1.10	1.10	1.10	1.20
12	0.22	0.30	0.41	0.44	0.50	0.67	0.60	0.77	0.77
10	0.13	0.18	0.25	0.30	0.30	0.40	0.40	0.55	0.53
8	0.078	0.0980	0.14	0.16	0.17	0.23	0.21	0.27	0.31
6	0.034	0.0460	0.063	0.073	0.082	0.103	0.098	0.125	0.15
4	0.012	0.0150	0.021	0.025	0.0275	0.033	0.031	0.044	0.047
3	0.054	0.0610	0.010	0.0115	0.0123	0.015	0.014	0.021	0.021
2	0.020	0.0240	0.027	0.032	0.0345	0.040	0.0046	0.0077	0.0071
1.5	0.0091	0.0110	0.0135	0.0155	0.0170	0.021	0.0255	0.0275	0.0310
1.2		0.0061	0.0074	0.0080	0.0091	0.0118	0.0140	0.0150	0.0180
1.0				0.0046	0.0055	0.0072	0.0081	0.0092	0.0108
0.8							0.0040	0.0049	0.0058

Kr, the measurements of Rustgi *et al.*[23] and of Lukirskii *et al.*[24] The former measurements indicate that as in the case of Ar the calculated cross section is too high near threshold by a factor of 2 and drops off too rapidly, relative to the measured value. The calculated $3d$-ϵf cross section is in excellent agreement with the calculation of Cooper and Manson, and here the measurements of Lukirskii *et al.* indicate the cross section is too high by a factor of 2 at the maximum.

In Fig. 6 we show the calculated cross section of Xe and the measurements of Samson,[25] Ederer,[26] and Lukirskii *et al.*[27] The calculations are in good agreement with those of Cooper and Manson. Once again, the measurements of Samson on the $5p$-ϵd and Ederer on the $4d$-ϵf cross sections show that the calculated values are high at threshold by a factor of 2 and drop off too rapidly. However, the

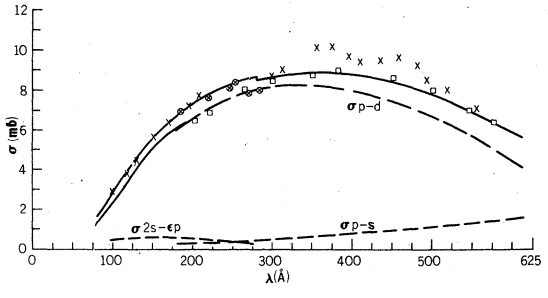

Fig. 3. The photo-ionization cross section of Ne from 100 to 625 Å. The squares are from Ref. 19 while the crosses and circled crosses are from Ref. 18.

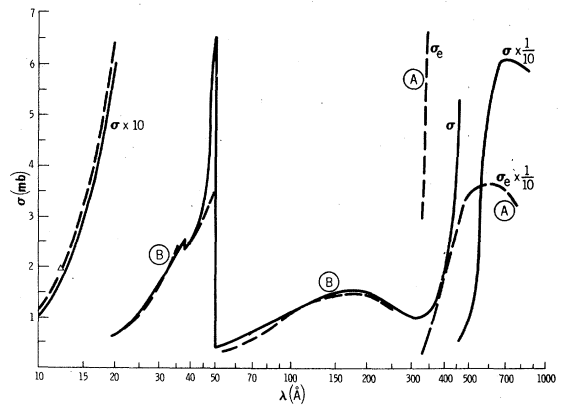

Fig. 4. The photo-ionization cross section of Ar from 10 to 800 Å. Dashed curve *A* is from Ref. 20, dashed curve *B* is from Ref. 21, and the triangle is from Ref. 22.

TABLE VI. Calculated cross sections for the elements Ni–Kr.

λ(Å)	Ni	Co	Zn	Ga	Ge	As	Se	Br	Kr
2000				13.0					
1500	2.60	0.87		66.60	28.0	49.0			
1200	1.10	0.32	1.50	3.30	16.2	33.0	63.5		
1000	0.30	0.08	0.40	3.40	8.90	22.7	48.5	60.0	
800	0.01	4.07	0.05	0.70	5.50	13.0	27.0	34.0	60.0
600	3.08	5.55	3.70	0.10	1.18	4.1	8.2	15.2	7.2
400	4.15	7.30	6.10	2.35	0.30	1.0	1.6	2.5	1.75
300	7.10	8.90	8.30	4.05	1.65	0.21	0.50	1.0	1.05
200	8.90	10.2	9.90	7.70	5.10	1.53	0.04	0.35	0.75
150	9.50	10.1	9.40	8.90	7.40	5.25	3.10	1.0	0.70
120	7.70	8.15	8.45	8.65	8.20	7.62	6.00	3.0	1.2
100	6.75	7.15	7.05	7.55	7.85	7.40	7.50	6.4	3.4
800	5.35	5.80	5.75	6.35	6.80	7.10	7.10	7.75	6.1
60	3.40	4.00	3.80	4.90	5.50	5.70	6.25	7.35	6.8
40	1.50	1.70	1.85	2.55	3.30	3.22	3.55	4.1	4.4
30	0.85	0.95	1.07	1.40	2.10	1.88	2.00	2.3	2.65
20	0.39	0.43	0.44	0.52	0.64	0.68	0.75	0.78	0.95
15	0.19	0.21	0.21	0.28	0.34	0.37	0.40	0.46	0.54
12	0.90	1.00	1.06	0.16	0.20	0.22	0.245	0.285	0.34
10	0.60	0.67	0.66	0.78	0.91	0.145	0.15	0.185	0.22
8	0.34	0.39	0.42	0.51	0.58	0.640	0.60	0.620	0.70
6	0.16	0.19	0.195	0.23	0.27	0.32	0.38	0.375	0.41
4	0.052	0.065	0.075	0.075	0.085	0.11	0.115	0.120	0.14
3	0.025	0.030	0.0285	0.036	0.040	0.049	0.052	0.054	0.061
2	0.0082	0.010	0.0094	0.012	0.0135	0.017	0.018	0.0185	0.020
1.5	0.0035	0.0045	0.0042	0.0053	0.0061	0.0077	0.0084	0.0085	0.0096
1.2	0.0207	0.0235	0.025	0.0270	0.0033	0.0039	0.0046	0.0045	0.0053
1.0	0.0125	0.0145	0.0155	0.0170	0.0190	0.0230	0.0027	0.0027	0.0032
0.8	0.0065	0.0072	0.0083	0.0093	0.0106	0.0118	0.0137	0.0165	0.0205
0.6			0.0036	0.0042	0.0047	0.0050	0.0058	0.0069	0.0079
0.4							0.0019	0.0020	0.0022

measurements of Lukirskii indicate that beyond the zero in the $4d$-ϵf cross section the calculations are in good agreement with experiment.

It is often assumed that for wavelengths less than 10 Å the cross section measured on a solid should agree with that for a free atom. To determine if 10 Å is too conservative a figure we have compared our calculated atomic cross sections with measurements made on solids and on simple gaseous molecules.

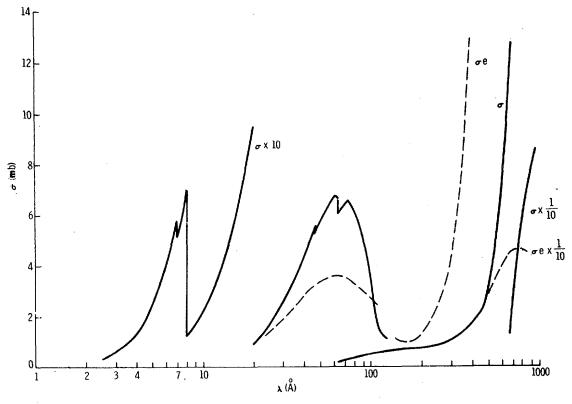

Fig. 5. The photo-ionization cross section of Kr from 3 to 1000 Å. The dashed curve above 100 Å is from Ref. 23 and below 100 Å from Ref. 24.

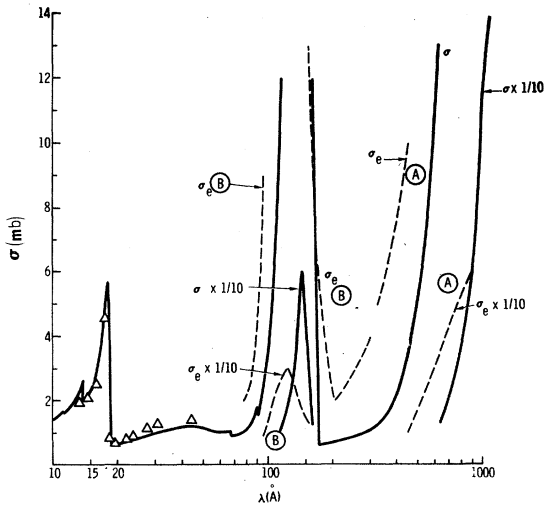

Fig. 6. The photo-ionization cross section of Xe from 10 to 1000 Å. Dashed curve A is from Ref. 25, dashed curve B from Ref. 26, and the triangles from Ref. 27.

TABLE VII. Calculated cross sections for the elements Rb–Rh.

λ (Å)	Rb	Sr	Y	Zr	Nb	Mo	Tc	Ru	Rh
2000	0.0050	0.400	1.0	1.80	0.54	0.70		1.05	1.35
1500	0.0020	0.026	3.0	0.30	8.5	0.10	0.73	0.18	0.32
1200	0.0075	0.002	4.3	6.0	11.0	11.4	0.20	0.02	0.0
1000	0.011	0.009	5.4	9.2	14.0	15.0	0.04	8.0	9.6
800	0.0145	0.039	6.4	12.8	17.5	20.5	8.4	11.5	13.5
600	0.0130	0.050	6.25	13.0	20.8	25.6	17.5	20.0	21.6
400	6.00	6.60	2.75	6.8	15.0	23.0	30.0	31.2	37.5
300	2.00	1.95	3.00	4.6	10.2	9.30	14.5	28.5	31.5
200	0.50	0.60	1.10	1.2	0.83	2.30	3.50	6.7	7.0
150	0.33	0.60	0.83	0.87	0.74	1.00	1.25	1.60	1.50
120	0.25	0.51	0.76	0.72	0.71	0.88	1.04	1.08	1.03
100	1.0	0.47	0.68	0.63	0.65	0.90	0.96	1.06	1.10
80	3.9	0.39	2.80	0.52	0.55	0.92	0.91	1.02	1.17
60	4.8	4.30	6.90	0.70	0.39	0.80	0.83	0.95	1.15
40	4.3	5.00	4.40	5.1	4.10	4.42	3.70	0.75	1.10
30	2.65	3.40	3.25	3.95	4.32	4.04	4.50	3.73	4.52
20	1.25	1.60	1.50	2.00	2.40	2.13	2.40	2.85	2.55
15	0.77	0.90	0.83	1.06	1.32	1.15	1.25	1.42	1.45
12	0.50	0.57	0.50	0.68	0.80	0.70	0.75	0.87	0.92
10	0.30	0.40	0.40	0.48	0.53	0.46	0.49	0.60	0.60
8	0.16	0.265	0.235	0.31	0.33	0.25	0.29	0.32	0.31
6	0.48	0.470	0.140	0.18	0.175	0.125	0.150	0.155	0.155
4	0.16	0.210	0.220	0.27	0.30	0.280	0.295	0.310	0.285
3	0.080	0.105	0.115	0.135	0.135	0.125	0.132	0.140	0.172
2	0.029	0.044	0.045	0.050	0.050	0.041	0.045	0.048	0.058
1.5	0.014	0.023	0.024	0.025	0.024	0.019	0.0215	0.0235	0.027
1.0	0.0049	0.0090	0.010	0.010	0.0089	0.0066	0.0077	0.0080	0.0092
0.8	0.0160	0.0056	0.0061	0.0059	0.0051	0.0037	0.0044	0.0045	0.0051
0.6	0.0088	0.0117	0.0120	0.0130	0.0122	0.0120	0.0160	0.0022	0.00235
0.4	0.0027	0.0035	0.0041	0.0042	0.0042	0.0042	0.0047	0.0051	0.0054
0.3	0.00115	0.0015	0.00215	0.0020	0.00175	0.00185	0.0022	0.0022	0.0025

In Fig. 7 we show the calculated cross section for Al, and the measurements of Tomboulian and Pell,[28] Fomichev and Lukirskii,[29] Ogier, Lucas, and Park,[30] and Cooke and Stewardson.[31] With the exception of the measurements of Tomboulian and Pell, the other sets of measurements, made on a solid, are in excellent agreement with the calculation.

In Fig. 8, we show the calculated cross section for Ag down to 10 Å and the measurements of Haensel *et al.*,[32] of Lukirskii *et al.*,[33] and of Cooke

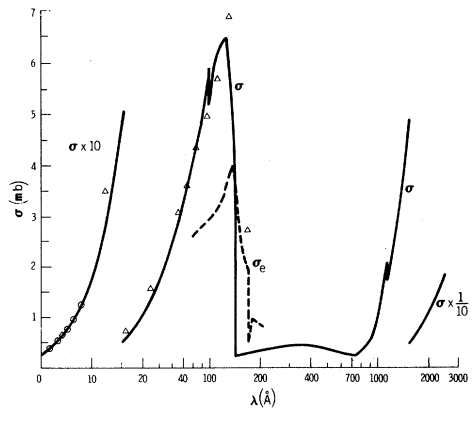

Fig. 7. The photo-ionization cross section of Al from 10 to 2500 Å. The dashed curve is from Ref. 28, the triangles from Ref. 29, the circles from Ref. 31, and the square from Ref. 30.

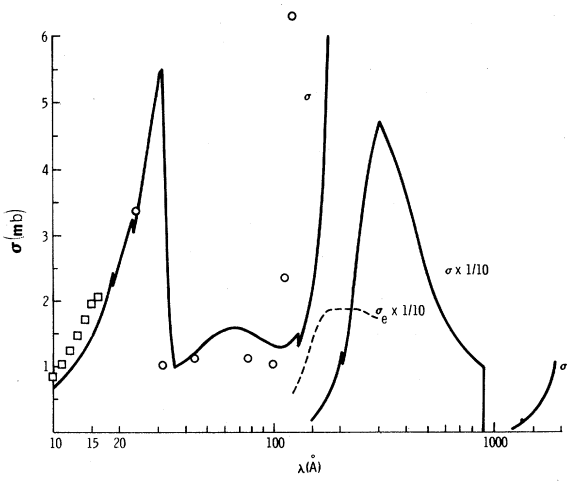

Fig. 8. The photo-ionization cross section of Ag from 10 to 1900 Å. The dashed curve is from Ref. 32, the circles from Ref. 33, and the squares from Ref. 30.

TABLE VIII. Calculated cross sections for the elements Pd–Xe.

λ(Å)/Element	Pd	Ag	Cd	In	Sn	Sb	Te	I	Xe
2000				11.0	42.0				
1500	12.5	0.28	1.60	5.6	21.0	56.5			
1200	17.8	0.04	0.44	2.75	12.0	30.0	65.0	16.	
1000	19.8	9.0	0.10	1.85	7.10	16.5	31.0	65.0	110.
800	22.9	11.5	0.0	0.86	3.70	8.0	14.0	23.5	37.0
600	28.0	17.1	10.1	0.44	1.65	2.55	4.70	7.60	10.6
400	36.0	37.0	29.0	6.00	0.58	0.86	1.43	2.07	2.2
300	34.0	46.5	42.9	31.5	23.0	0.55	0.950	1.32	1.1
200	12.8	11.0	16.0	28.3	21.0	20.0	17.0	3.20	0.67
150	2.90	2.13	5.00	7.30	8.2	18.5	17.0	40.0	48.
120	1.10	1.37	1.70	1.60	4.2	2.60	2.35	6.60	14.
100	1.00	1.32	1.24	1.25	1.85	2.25	2.03	3.00	2.5
80	1.00	1.50	1.26	1.45	2.3	1.95	1.66	1.70	1.1
60	1.07	1.55	1.30	1.60	2.1	2.10	2.18	1.80	1.0
40	0.92	1.10	1.09	1.12	1.35	2.15	1.95	1.95	1.15
30	4.10	5.45	0.92	1.00	0.92	1.25	1.22	1.43	1.0
20	2.60	2.60	3.45	3.65	3.00	7.00	6.30	7.20	0.63
15	1.62	1.42	2.20	2.42	2.15	2.72	3.05	2.40	2.30
12	1.10	0.94	1.38	1.50	1.38	1.83	2.10	1.85	1.80
10	0.70	0.67	0.88	0.90	0.80	1.20	1.20	1.23	1.37
8	0.38	0.32	0.54	0.55	0.54	0.75	0.74	0.69	0.86
6	0.175	0.155	0.26	0.26	0.275	0.39	0.38	0.36	0.42
4	0.300	0.175	0.077	0.087	0.092	0.130	0.140	0.117	0.15
3	0.170	0.190	0.200	0.230	0.260	0.240	0.290	0.048	0.071
2	0.53	0.065	0.065	0.072	0.080	0.079	0.091	0.093	0.110
1.5	0.024	0.030	0.030	0.033	0.038	0.037	0.043	0.041	0.051
1.0	0.053	0.0103	0.0093	0.011	0.0125	0.0125	0.0140	0.0132	0.0170
0.8	0.0046	0.0056	0.0049	0.0061	0.0069	0.0068	0.0077	0.0071	0.0090
0.6	0.0022	0.0026	0.0021	0.0028	0.0032	0.0031	0.0035	0.0034	0.0040
0.4	0.0059	0.0063	0.0067	0.0078	0.0082	0.0083	0.0095	0.0011	0.0013
0.3	0.0026	0.0029	0.0029	0.0034	0.0036	0.0038	0.0041	0.0046	0.0046
0.2		0.0010	0.0010	0.0011	0.0012	0.0013	0.0013	0.0015	0.0015

and Stewardson,[31] all made on solid Ag. Down to 100 Å the difference between the calculation and experiment is of the same type as that seen in Xe, i.e., the calculated $4d$-ϵf cross section. Below 100 Å the data of Lukirskii *et al.*, are in good agreement with the calculation (considering that the calculated zero of the $4d$-ϵf cross section occurs at a longer wavelength than the measurements indicate). The data of Cooke and Stewardson indicate the calculation is poor between 10 and 17Å. However, in Fig. 9, we show that below 10 Å the data of Cooke and Stewardson do not agree with that of Allen's tabulation,[22] the latter in excellent agreement with the calculation.

Lukirskii and Zimkina[21] have measured the cross section of gaseous C_2H_2OH over a wide spectral range. In Fig. 10 we compare their data with a sum of the calculated atomic cross sections (i.e., $6\sigma_H + 2\sigma_C + \sigma_0$). They are in excellent agreement from 25 to 250 Å. They differ at the carbon K edge because the model carbon $1s$ eigenvalue (– 22.0 Ry) is higher than the Herman-Skillman value (– 21.38 Ry) and thus the calculated cross section is too high at threshold. This excellent agreement led us to compare the sum of calculated atomic cross sections with measurements on some simple molecules (those for which data are available below 800 Å).

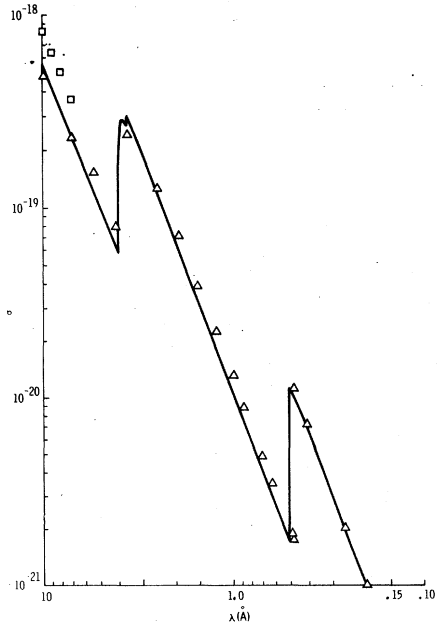

Fig. 9. The photo-ionization cross section of Ag from 0.2 to 10 Å. The squares are from Ref. 30 and the triangles from Ref. 22.

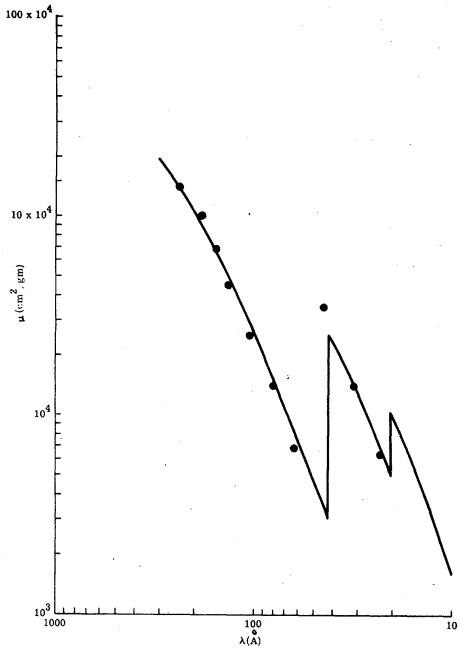

Fig. 10. The mass absorption coefficient of 2C + 6H + O from 10 to 250 Å. The solid circles are for C_2H_5OH taken from Ref. 33.

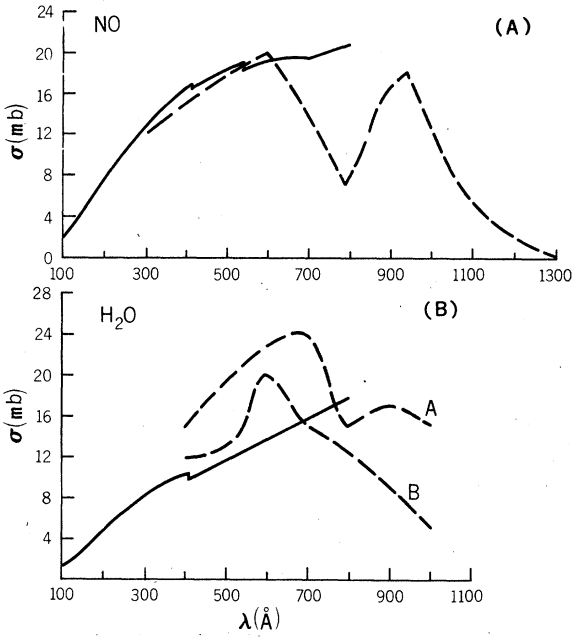

Fig. 12. The photo-ionization cross sections of N + O (A) and 2H + O (B) from 100 to 800 Å. The dashed curve for NO and dashed curve *A* are from Ref. 35 while dashed curve *B* is from Ref. 36.

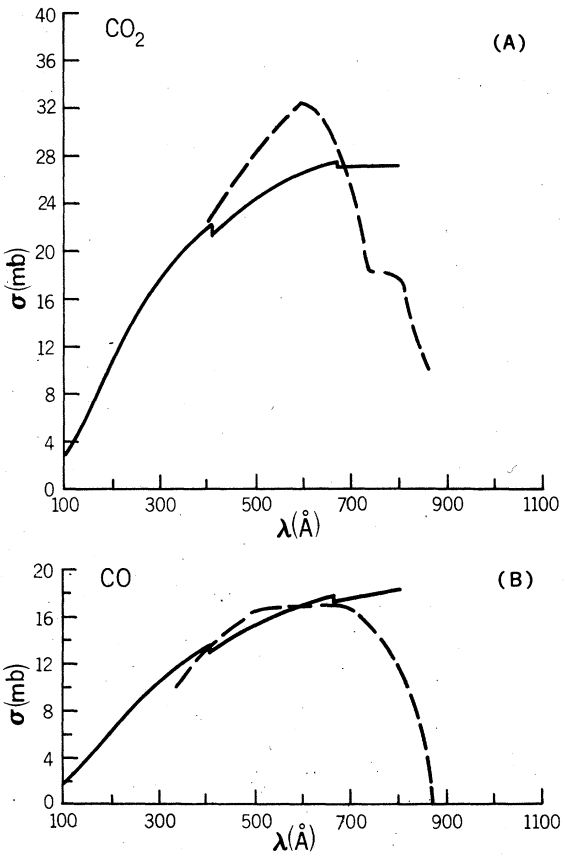

Fig. 11. The photo-ionization cross sections of C + 2O (A) and *C* + O (B) from 100 to 900 Å. The dashed curves are from Ref. 34.

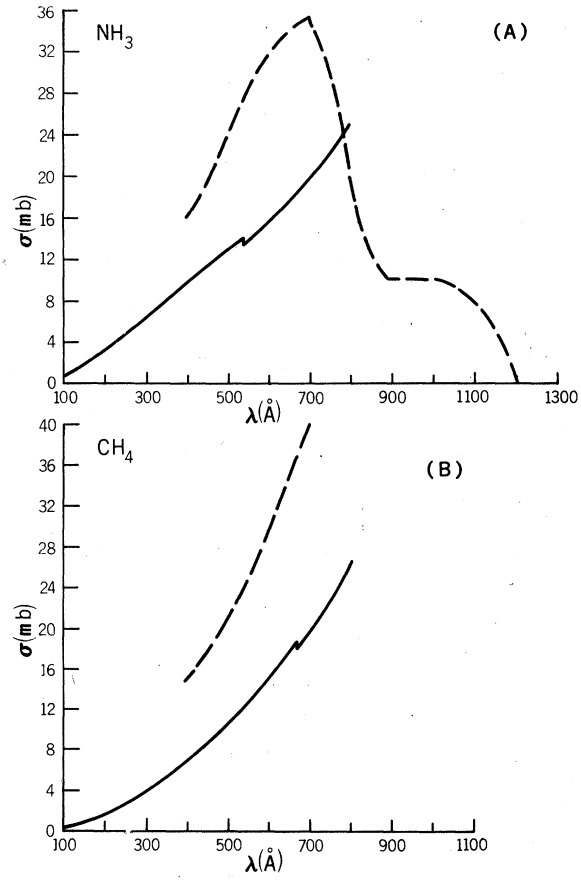

Fig. 13. The photo-ionization cross sections of N + 3H (A) and C + 4H (B) from 100 to 800 Å. The dashed curves are from Ref. 37.

In Fig. 11 we show the comparison for CO[34] and CO_2,[34] in Fig. 12 for NO[35] and H_2O,[35,36] and in Fig. 13 for NH_3[37] and CH_4.[37] For CO, CO_2, and NO the calculated and measured cross sections are in good agreement below 400 Å; for H_2O the experimental situation is not clear, while for NH_3 and CH_4 the cross sections below 400 Å agree in slope but differ in magnitude by a factor of 2. This is surprising for CH_4, since the agreement is so good for C_2H_5OH.

CONCLUSIONS

The calculated cross sections for the elements He–Mg are in good agreement with experiment. For the elements Al–Xe for the outermost d and p shells the calculated cross sections can be in error by a factor of 2 at threshold and with too rapid a slope down to a wavelength shorter than that at the zero of the d shell to continuum f cross section. Below this wavelength the calculations are in good agreement with experiment. The disagreement at longer wavelengths can be attributed to the breakdown of the independent-particle, common-central-potential assumption. These calculations were based on the assertion that the straight line approximation to the Herman-Skillman effective charge led to an accurate continuum orbital. The agreement of these calculations with those of Cooper and Manson, and with experimental measurements, indicates that the assertion is valid. We are currently using the model continuum orbitals to compute atomic fluorescence yields, and generalized oscillator strengths for ionization.

---

*This work was supported by the U. S. Atomic Energy Commission.

[1]E. J. McGuire, Phys. Rev. 161, 51 (1967).

[2]F. Herman and S. Skillman, Atomic Structure Calculations (Prentice-Hall, Inc., Englewood Cliffs, New Jersey, 1963). The Hartree-Fock-Slater results referred to throughout this paper are those of Herman and Skillman.

[3]H. Hall, Rev. Mod. Phys. 8, 358 (1936).

[4]The potential and boundary conditions on the hydrogen atom allow only these functions.

[5]E. E. Salpeter and M. H. Zaidi, Phys. Rev. 125, 248 (1962).

[6]J. W. Cooper, Phys. Rev. 128, 681 (1962).

[7]S. T. Manson and J. W. Cooper, Phys. Rev. 165, 126 (1968).

[8]See Ref. 2 (pp. 1-8). The model orbitals are in excellent agreement with those of Ref. 2 when the one-electron energies are the same. When these eneregies differ, the orbitals differ slightly in the tails.

[9]This is the grid size used in Ref. 2.

[10]The functions used in determining the eigenfunctions are defined in Ref. 1.

[11]T. Koopmans, Physica 1, 104 (1933).

[12]P. S. Bagus, Phys. Rev. 139, A619 (1965).

[13]A. Burgess and M. J. Seaton, Monthly Notices Roy. Astron. Soc. 120, 121 (1960).

[14]F. Wuilleumier, Compt. Rend. 257, 855 (1963).

[15]Complete tables of model parameters, eigenvalues, cross sections, and threshold jumps are available from the author.

[16]R. B. Cairns and J. A. R. Samson, Phys. Rev. 139, 1403 (1965).

[17]A. Dalgarno, R. J. W. Henry, and A. L. Stewart, Planetary Space Sci. 12, 235 (1964).

[18]D. L. Ederer and D. H. Tomboulian, Phys. Rev. 133, A1525, (1964).

[19]J. A. R. Samson, J. Opt. Soc. Am. 55, 935 (1965).

[20]J. A. R. Samson, J. Opt. Soc. Am. 54, 420 (1964).

[21]A. P. Lukirskii and T. M. Zimkina, Izv. Akad. Nauk USSR, Ser. Fiz. 27, 817 (1963) [English transl.: Bull. Acad. Sci. USSR., Phys. Ser. 808 (1963)].

[22]S. J. M. Allen, X Rays in Theory and Experiment edited by A. H. Compton and S. K. Allison (D. Van Nostrand, Co., Inc., Princeton, New Jersey, 1935), Appendix.

[23]O. P. Rustgi, E. I. Fisher, and C. H. Fuller, J. Opt. Soc. Am. 54, 745 (1964).

[24]A. P. Lukirskii, I. A. Brytov, and T. M. Zimkina, Opt. i Spektroskopiya 17, 438 (1964) [English transl.: Opt. Spectry. (USSR) 17, 234 (1964)].

[25]J. A. R. Samson, J. Opt. Soc. Am. 54, 842 (1964).

[26]D. L. Ederer, Phys. Rev. Lett. 13, 76 (1964).

[27]A. P. Lukirskii, I. A. Brytov and S. A. Gribovskii, Opt. i Spektroskopiya 20, 368 (1966) [English transl.: Opt. Spectry. (USSR) 20, 203 (1966)].

[28]D. H. Tomboulian and E. M. Pell, Phys. Rev. 83, 1196 (1951).

[29]V. A. Fomichev and A. P. Lukirskii, Opt. i Spectroskopiya 22, 796 (1967) [English transl.: Opt. Spectry. (USSR) 22, 432 (1967)].

[30]W. T. Ogier, G. J. Lucas, and R. J. Park, Appl. Phys. Letters 5, 146 (1964).

[31]B. A. Cooke and E. A. Stewardson, Brit. J. Appl. Phys. 15, 1315 (1964).

[32]R. Haensel, C. Kunz, and B. Sonntag, Phys. Letters 25A, 205 (1967).

[33]A. P. Lukirskii, E. P. Savinov, O. A. Ershov, and Yu. F. Shepelev, Opt. i Spektroskopiya 21, 310 (1964) [English transl.: Opt. Spectry. (USSR) 21, 168 (1964)].

[34]H. Sun and G. L. Weissler, J. Chem. Phys. 23, 1625 (1955).

[35]H. Sun and G. L. Weissler, J. Chem. Phys. 23, 1372 (1955).

[36]Measurement A on H_2O taken from Ref. 33. Measurement B is taken from E. W. McDaniel, Collision Phenomena in Ionized Gases (John Wiley & Sons, Inc., New York, 1964).

[37]H. Sun and G. L. Weissler, J. Chem. Phys. 23, 1160 (1955).